

Received February 7, 2020, accepted February 13, 2020, date of publication February 20, 2020, date of current version March 3, 2020.

Digital Object Identifier 10.1109/ACCESS.2020.2975241

Detection of Interference Constraint Violation Based on Heterogeneous Data Fusion in Satellite-Earth Integrated Networks

NING YANG^{ID1}, PINGHUI LI^{ID1}, DAOXING GUO^{ID1}, (Member, IEEE), LINYUAN ZHANG^{ID2}, AND GUORU DING^{ID1}, (Senior Member, IEEE)

¹College of Communications Engineering, Army Engineering University of PLA, Nanjing 210007, China

²Jiangnan Institute of Computing Technology, Wuxi 214146, China

Corresponding author: Daoxing Guo (xyzgfg@sina.com)

This work was supported in part by the Natural Science Foundation for Distinguished Young Scholars of Jiangsu Province under Grant BK20190030, in part by the National Natural Science Foundation of China under Grant 61871398 and Grant 61931011, in part by the National Key Research and Development Program of China under Grant 2018YFB1801103, and in part by the Equipment Advanced Research Field Foundation under Grant 61403120304.

ABSTRACT In the downlink scenario of satellite-earth integrated networks, the secondary systems ought to share spectrum resources with no extra interference on the primary system under the premise of interference constraints. However, due to various factors, e.g., equipment failure or selfish drive, interference constraint violation (ICV) exists, which seriously threatens the reliable communication of primary systems. Therefore, effective detection of the secondary users' working status is necessary to protect the communication of primary user. In this paper, a new geolocation spectrum database is introduced to coordinate the information interaction for spectrum usage and surveillance, and a detection framework is proposed to detect the ICV behaviors, which utilizes the generalized likelihood ratio test and maximum a posterior to determine the transmitted power of the secondary users. Moreover, a data fusion scheme based on sensing node selection is designed to alleviate negative effects on the detection performance brought by the existence of the primary user. Furthermore, the test statistics are derived under different channel models. Finally, extensive simulations are provided to verify the proposed framework under various parameter configurations.

INDEX TERMS Satellite communication, spectrum sharing, interference constraints, generalized likelihood ratio test.

I. INTRODUCTION

A. BACKGROUND AND MOTIVATION

The difficulty of spectrum detecting in the satellite-earth integrated networks is positively correlated with its spectrum sharing dimension, that is, with the increase of its spectrum sharing dimension, the spectrum utilization will be more sufficient, and the spectrum efficiency will be improved [1]–[8]. However, the increase of sharing dimension means the exponential increase of information needed to evaluate the spectrum usage behavior, and the difficulty of obtaining and analyzing the spectrum information increases accordingly.

In fact, to enhance the spectrum efficiency of the satellite-earth integrated networks, more refined space-time spectrum sharing strategies based on spectrum heterogeneous characteristics of space and time can be designed, i.e., ground

systems at different locations and times can access the spectrum in interference-free or interference-tolerant ways, respectively. In the communication area of the primary user, the secondary users should choose to access the channel only when the primary user is absent, so that there will be no interference to the communication of the primary user. While outside the communication area of the primary user, the secondary users can access channel when the primary user is active, but the behavior of secondary user can produce interference to the satellite earth station, especially the closer the secondary user is to the satellite earth station, the stronger the interference will be. Therefore, in order to achieve reliable communication, it is necessary to control the transmitted power of the secondary user to ensure that the interference to the primary user's communication is within a certain range.

In summary, the spectrum opportunities are space-time heterogeneous for secondary users [9], which means that the interference constraints on opportunistic access are different.

The associate editor coordinating the review of this manuscript and approving it for publication was Faissal El Bouanani^{ID}.

Interference constraints are established from the perspective of the primary user [10]. Specifically, when the primary user is not working, interference constraints can be ignored, and secondary users can freely access the channel [11]. When the primary user is working, secondary users are not allowed to exist in the communication area of the primary user, and the communication protection belt allows secondary users to access, but the transmitted power must be controlled appropriately to control the interference in an acceptable range [12].

B. RELATED WORK

Interference constraint is the premise that the primary user authorizes the secondary user to share the spectrum. However, some secondary users may break these constraints to improve their communication benefits and cause intolerable interference to the communication of the primary user, that is, the violation of interference constraint occurs. Existing studies of detection of interference constraint violation mainly focus on the joint detection and estimation of abnormal spectrum usage [13]–[16] or the study of interference avoidance [17] in the spectrum sharing scenario. In [13], breaking the priority schedule of spectrum access is defined as opportunistic illegal access and generalized multi-hypothesis Neyman-Pearson (GMNP) criterion is used to detect spectrum opportunity [18] and illegal access in the terrestrial networks. In [14], the transmitted power violation is modeled as a hybrid binary hypothesis testing problem, which strengthens the communication of other secondary users instead of primary user. Similarly, to determine whether the secondary user is working legally, the authors focus on solving the problem called primary user emulation attack in [15]. In [16], aiming at deriving the maximum permissible transmitted power, the authors formulate the problem of spatial spectrum sensing as the estimation of the location and transmission power of the primary transmitter. In [17], the impact of secondary transmissions on a primary receiver is studied in terms of interference probability. Note that in those studies, the spectrum sharing scenario mainly focus on terrestrial networks rather than satellite-earth integrated networks.

While in the satellite-earth spectrum sharing scenario, the concept of cognitive satellite terrestrial radios for satellite-earth integrated systems has been presented in [19]. In [8], when geostationary (GEO) satellite is regarded as the primary user and non-geostationary (NGEO) satellite as the secondary user, the spectrum sharing of the primary user is analyzed in temporal domain, where secondary users are regarded as interference sources, and the concept of protected area is proposed to guarantee the communication of primary users by accumulating the interference of ground base stations to satellite terminals. In [20], interference model between ground base station (BS) and satellite terminal is carried out according to the interference power level. Similarly, in [7], the power levels available to secondary users are derived by analyzing the interference caused by N GEO systems to

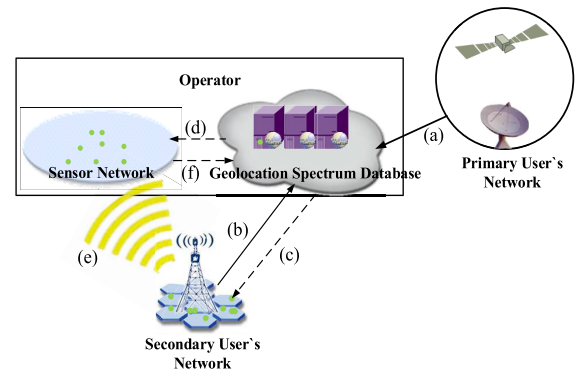


FIGURE 1. Basic operational process of geolocation spectrum database. (a) Report its information to geolocation spectrum database; (b) Forward the enquiry to geolocation spectrum database; (c) Feed back the spectrum availability information to the secondary user; (d) Send the information of the secondary user and the primary user to the sensor network; (e) The process of detection; (f) Report detecting results.

GEO systems, respectively, both in the downlink and uplink. Note that in those studies, there are some studies analyzing the interference but few on detection of interference constraint violation in the satellite-earth integrated networks.

To the best of the authors' knowledge, there is no existing work considering the detection of ICV in the scenario of satellite-earth integrated spectrum sharing networks. Therefore, from the perspective of strengthening the primary user's detection, it is of great significance to propose and study the behavior of interference constraint violation.

C. CONTRIBUTIONS

In this paper, a joint detecting framework is built, where every sensing node makes spectrum sensing, and based on the signals received from the sensors, the fusion center makes data fusion and global decision, just as shown in Fig. 1. Our aim is to detect whether the secondary user violates the interference constraints. On the detection of ICV in the scenario of satellite-earth integrated spectrum sharing, this paper makes following contributions:

- Propose a new geolocation spectrum database framework, in which the roles and tasks of the primary user, the secondary users and the sensor network in spectrum sharing are specified. Specifically, the sensor network is introduced in this framework to perform the detection of ICV.
- Formulate a generalized model for spectrum sharing in the satellite-earth integrated networks, which can reflect the combined effects of heterogeneous spectrum sharing and interferences, and further the model of space-time heterogeneous ICV is established.
- Analyze the influence of secondary user's transmitted power, position information and channel on detection, by deducing the detector of ICV.
- Develop a detecting framework based on heterogeneous data fusion, where the sensing data is weighted based on sensor selection by calculating signal to interference plus noise ratio (SINR) at every sensing node instead of trusting all sensing data.

- Provide comprehensive simulations under various parameter configurations, which demonstrates that the proposed detecting framework is quite effective and significantly mitigates the effect of useless sensing data.

The reminder of this paper is organized as follows. The system model of ICV is formulated in Section II. Section III derives the test statistics under different channels, and further gives a detecting framework based on heterogeneous data fusion. Simulation is given in Section IV, followed by the conclusion in Section V.

II. SYSTEM MODEL

A. HETEROGENEOUS SPECTRUM SHARING MODEL WITH GEOLOCATION SPECTRUM DATABASE

In this paper, space-time spectrum sharing strategy is considered, that is, not only the time domain spectrum opportunity, but also the space domain spectrum opportunity is utilized by controlling the transmitted power of the secondary user to access the channel when the primary user is working according to the distance between the secondary user and the primary user. Therefore, heterogeneous spectrum sharing can be realized due to different spectrum opportunities in different locations of secondary users. What's more, this paper utilizes the geolocation spectrum database [21]–[23] to facilitate the spectrum sharing. Therefore, it is reasonable to assume that the location information of each secondary user is available for the sensor network, but its working status is unknown. As shown in Fig. 1, in fact, the sensor network is constituted by the sensing nodes and the fusion center, and the detailed process of geolocation spectrum database can be summarized as:

- The primary user sends its information to geolocation spectrum database so as to calculate the maximum transmitted power of the secondary user when there is a need for sharing;
- The secondary user forwards the sharing enquiry to the database during which time its location information needs to be reported;
- The database calculates the set of vacant frequency band(s) at the location of that secondary user using a combination of radio signal propagation models, terrain data, and up-to-date parameters of the working transmitters, and then feeds back the spectrum availability information and corresponding power constraint to that secondary user;
- The database sends the information of the secondary user and the primary user to the sensor network for the detection of the usage of spectrum;
- The sensor network determines whether the secondary user violates the interference constraint through continuous data collection and estimation;
- The sensor network reports its detecting results to the database.

Therefore, this assumption is reasonable in the case of the spectrum sharing with geolocation spectrum database.

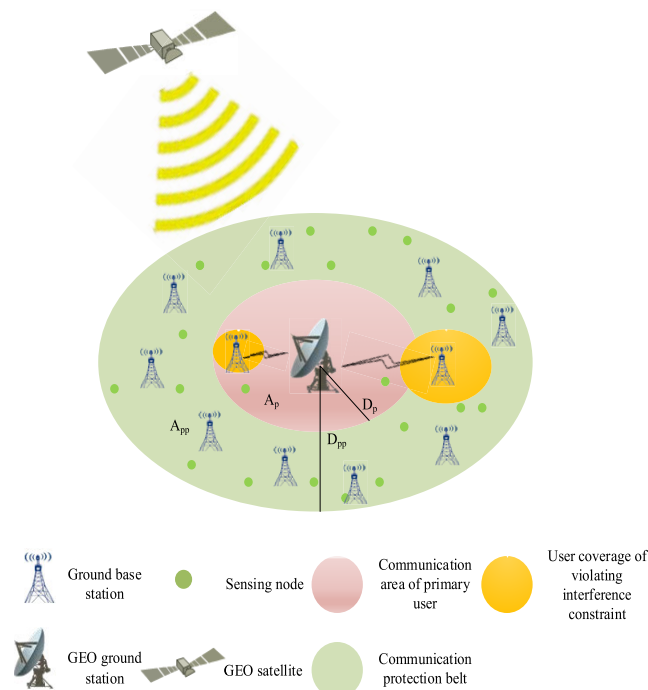


FIGURE 2. Model of Heterogeneous ICV.

As shown in Fig. 2, GEO satellite and GEO ground station denote the primary user transmitter and the primary user receiver, respectively. The space is divided into three regions:

- *The primary user communication area* is denoted by A_p as the possible distribution range of the GEO ground station at the perspective of the secondary user (ground base station) with a radius of D_p , where the primary user receiver can normally receive signals. Therefore, when the primary user is working, the secondary user is not allowed to access the channel. User coverage of violating interference constraint represents the communication range of user who violates interference constraint.
- *The communication protection belt* is represented by A_{pp} and the radius of the edge is D_{pp} , where the primary user's signal is weak. The primary user receiver cannot receive the channel normally, but the secondary user can perceive the primary user's signal. In order to protect the communication of the primary user from interference, when the primary user is working, the secondary user needs to control the transmitted power to make the interference on the primary user receiver that may appear at the edge of the primary user communication area controllable.
- *The white area of spectrum opportunity* is denoted by the area that D_{pp} away from the primary user. The secondary users in this area cannot effectively interfere with the communication of the primary user even if they are working at the highest power. Therefore, they can freely access the channel and their communication is not subject to interference. Therefore, it is not considered in this paper.

Finally, when the primary user is working, the spectrum sharing method can be expressed as follows:

$$\mathcal{N} : y_k(m) = \sqrt{P_{0,k}}u(m) + \sqrt{P_{j,k}}s_j(m) + n_k(m),$$

$$P_j \leq g(D_j), \quad L_j \in A_{pp}, \quad (1)$$

where the primary user and the secondary users work on the same channel, with $y_k(m)$ as the sensing data of the k -th sensing node at the m -th sampling point, $P_{0,k}$ and $P_{j,k}$ as the signal received power of the primary user and the secondary user at the k -th sensing node, respectively, $n_k(m)$ as additive white gaussian noise (AWGN), $u(m)$ and $s_j(m)$ as the signal of the primary user and the j -th secondary user with the transmitted power P_j . The relationship between the received power $P_{j,k}$ and the secondary user transmitted power P_j can be written as

$$P_{j,k} = h_{j,k}^2 P_j \quad j = 1, 2, \dots, J, \quad (2)$$

where $h_{j,k}$ denotes the channel gain between the k -th sensing node and the j -th secondary user, J represents the number of secondary users distributed in the primary user communication area and communication protection belt. The relationship between the received power $P_{0,k}$ and the primary user transmitted power P_0 can be written as [24]

$$P_{0,k} = P_0 G_{0,k}(\theta_{0,k}) \left(\frac{c}{4\pi f_c d_{0,k}} \right)^2, \quad (3)$$

where P_0 represents the transmitted power of the primary user (satellite), $P_{0,k}$ denotes the signal received power of the primary user at the k -th sensing node and $G_{0,k}(\theta_{0,k})$ represents the antenna gain of the satellite at the direction of $\theta_{0,k}$, with $d_{0,k}$ as the distance between the transmitter of primary user and the k -th sensing node. As shown in Fig. 3, $h = 35786\text{Km}$ is the orbital altitude of the satellite. $\theta_{0,k}$ is the off-axis angle of the GEO satellite in the direction of the k -th sensing node and can be further calculated by $\theta_{0,k} = \arctan(\frac{d_{0,k}}{h})$. Moreover, the GEO satellite antenna gain $G_{0,k}(\theta_{0,k})$ refers to the standard in ITU-R.S.672-4 [25] and can be described as

$$G_{0,k}(\theta_{0,k}) = \begin{cases} G_{s,\max} - 3\left(\frac{\theta_{0,k}}{\theta_{s,b}}\right)^2, & \theta_{s,b} < \theta_{0,k} < b\theta_{s,b}, \\ G_{s,\max} + L_n, & b\theta_{s,b} < \theta_{0,k} < c\theta_{s,b}, \\ G_{s,\max} + L_n + 20 - 25 \log\left(\frac{\theta_{0,k}}{\theta_{s,b}}\right), & c\theta_{s,b} < \theta_{0,k} < \theta_1, \\ 0, & \theta_1 < \theta_{0,k} < 90^\circ, \\ 3, & 90^\circ < \theta_{0,k} < 180^\circ, \end{cases} \quad (4)$$

where $G_{s,\max} = 47\text{dBi}$ is the maximum gain of the GEO satellite antenna, $\theta_{s,b}$ is the one half the 3 dB beamwidth, L_n is the desired side-lobe level relative to peak gain, and θ_1 is the value of $\theta_{0,k}$, when Eq. (5) is valid. For $L_n = -20$, the values of b and c are 2.58 and 6.32, respectively.

$$G_{0,k}(\theta_{0,k}) = G_{s,\max} + L_n + 20 - 25 \log\left(\frac{\theta_{0,k}}{\theta_{s,b}}\right) = 0\text{dB}. \quad (5)$$

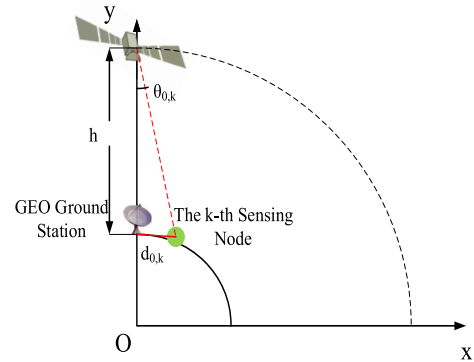


FIGURE 3. The description of $\theta_{0,k}$.

It is reasonable to assume that there is access control between secondary users so that the communication ranges of working secondary users does not overlap. $L_j \in A_{pp}$ means that the secondary user can only work in the communication protection belt and meet the transmitted power constraint, i.e.,

$$P_j \leq g(D_j), \quad (6)$$

where

$$g(D_j) = \begin{cases} 0, & D_j \leq D_p, \\ I_{th}(D_j - D_p)^\alpha, & D_p \leq D_j \leq D_{pp}, \end{cases} \quad (7)$$

with $D_j = \|L_0 - L_j\|$ as the distance between the secondary user and the primary user receiver where $L_0 = (x_0, y_0)$ and $L_j = (x_j, y_j)$ denote the location of primary and secondary users, respectively, I_{th} as the interference constraint at the edge of the primary user communication area, α as the path fading factor.

B. MODEL OF ICV

High efficient spectrum utilization is premised on the strict adherence of secondary users to interference constraints. However, in practice, due to a variety of reasons, such as inaccurate channel perception, equipment failure, or selfish drive, the secondary user may violate the interference constraint and cause the communication of the primary user to be blocked, which is called ICV. In particular, corresponding to the spatial heterogeneity characteristic of interference constraint in the heterogeneous spectrum sharing in Eq. (1), ICV also reflects the spatial heterogeneity characteristic. Specifically, from the perspective of interference control of primary user communication, when the primary user is working, it can be divided into two kinds of ICVs according to the region where the secondary user is located at.

1) In the communication area of the primary user, in order to protect the operation of the primary user receiver, the interference constraint is zero tolerance, that is, the secondary users are not allowed to access the channel. At this time, if one secondary user accesses the channel without permission, and such behavior directly will interfere the primary user receiver, resulting in the failure of receiving the primary user signal.

2) Within the communication protection belt, interference constraint is to set the transmitted power of secondary users,

but at this point, the secondary users access channel break-through the limitation of transmitted power, working with a higher transmission power, i.e., $P_j > g(D_j)$. In result, the secondary users can gain higher communication proceeds, but would lead to strong interference on the primary user's receiver, especially one at the edge of the primary user communication area, which always means the communication failure.

The above two kinds of ICVs are respectively modeled as follows:

$$\begin{cases} \mathcal{F}_0 : y_k(m) = \sqrt{P_{0,k}}u(m) + \sqrt{P_{j,k}}s_j(m) \\ \quad + n_k(m), \quad D_j < D_p, \\ \mathcal{F}_1 : y_k(m) = \sqrt{P_{0,k}}u(m) + \sqrt{P_{j,k}}s_j(m) \\ \quad + n_k(m), \quad P_j > g(D_j), D_p \leq D_j \leq D_{pp}. \end{cases} \quad (8)$$

Among them, the received power of sensing nodes depends on the transmitted power and relative the location of sensing nodes and secondary users. It is analyzed in detail with different channel models in Section III.

It can be seen that, ICV is spatially heterogeneous, which is consistent with the heterogeneous spectrum sharing. Specially, in the primary user communication area, detecting whether the secondary users are working is enough to determine the existence of the ICV behaviors; while in the communication protection belt, when the secondary user is detected to be working, the upper limit of its transmitted power should be inferred according to the position of the secondary user, and ICV should be determined according to the estimated value of the actual transmitted power. Therefore, the detection of ICV is built on the combination of the spectrum usage rules about interference constraints and the acquisition of position and power information.

III. DETECTION SCHEME BASED ON HETEROGENEOUS DATA FUSION

In this section, first of all, from the perspective of joint detection and estimation, this paper derives the detection method of ICV and the transmitted power estimation method for single secondary user, and then, considers the scenario in which multiple secondary users work simultaneously in the communication belt. In order to minimize the negative impact of other secondary users, primary user signals and noise on the accuracy of detection and estimation, a detection method based on node selection mechanism was developed.

A. ICV DETECTION IN SCENARIOS WITH SINGLE SECONDARY USER

As shown in Fig. 1, this paper considers that the location information of each secondary user is available for the sensor network, but its working status is unknown. In addition, it can estimate the position of the secondary user through the received power of the sensing node. In particular, when it detects ICV behavior of a certain secondary user, it can also accurately identify the secondary user. In this subsection, only one secondary user working scenario is considered in the

primary user communication area, i.e., $j = 1$, while detection in multi-user working scenario in the communication belt is considered later. At this point, the satellite system needs to determine whether the secondary user is working or not, and if it is, where. If the secondary user works in the communication area of the primary user, ICV is directly determined. If the secondary user is working in the communication protection belt, the power restriction at the position is further combined to determine whether the power constraint has been violated. Therefore, the detection of ICV can be divided into two parts: one is to find the position of the secondary user in the working state; the other is to determine whether the working secondary user violates the interference constraint. Therefore, the detector is deduced as follows. On the choice of the signal detector used by the sensing nodes, since the secondary user does not have a specific modulation mode, the feature detector cannot be used. In this paper, the simple and feasible energy detector is considered. Therefore, the test statistic T_k at node k can be approximately expressed as Gaussian Distribution according to the Central Limit Theorem [26] and can be written as

$$T_k \sim \begin{cases} \mathcal{N}\left(P_{0,k} + N_k, \frac{(P_{0,k} + N_k)^2}{M}\right), & \mathcal{H}_0 \\ \mathcal{N}\left(P_{0,k} + P_{1,k} + N_k, \frac{(P_{0,k} + P_{1,k} + N_k)^2}{M}\right), & \mathcal{H}_1 \end{cases} \quad (9)$$

where \mathcal{H}_0 and \mathcal{H}_1 indicate that the secondary user is not working or working, respectively, and N_k is the noise variance at the node k . The optimization criterion is to maximize the detection probability under the given false alarm probability. Therefore, when the received power of secondary users at each node is known, the optimal detection method is likelihood ratio test (LRT) [27], i.e.,

$$L(T) = \frac{p(T|P_t \neq 0)}{p(T|P_t = 0)} \underset{d_H = \mathcal{H}_0}{\overset{d_H = \mathcal{H}_1}{>}} \lambda, \quad (10)$$

where $P_t = \{P_{1,1}, P_{1,2}, \dots, P_{1,K}\}$ is the received power at all sensing nodes from the secondary user, $T = \{T_1, T_2, \dots, T_K\}$ is the test statistics at all sensing nodes, d_H denotes the result of judgment of secondary user's working status, i.e., $d_H \in \{0(\mathcal{H}_0), 1(\mathcal{H}_1)\}$, and λ is the detection threshold, which meets the following false alarm probability requirement

$$P_f = \int_{T:L(T) > \lambda} p(T|P_t = 0) dT. \quad (11)$$

However, the power and channel information of the secondary users are often unknown, so it is difficult to achieve the detection of spectrum usage of the secondary users through following the optimal detection criterion. For this mixed hypothesis testing problem with unknown parameters, the commonly used method is generalized likelihood ratio

test (GLRT), i.e.,

$$L_G(T) = \frac{p(T|\hat{P}_1, L_1, \mathcal{H}_1)}{p(T|P_1 = 0, \mathcal{H}_0)}, \quad (12)$$

where $\hat{P}_1 = \arg \max_{P_1} p(T|P_1, L_1, \mathcal{H}_1)$, with \hat{P}_1 as the estimate of the transmitted power P_1 of the secondary user, and L_1 as the location of the target secondary user. Since \hat{P}_1 is the unconstrained maximum likelihood estimation in the parameter space, it reaches the lower limit of Cramer-Rao, that is, it satisfies

$$\frac{d \ln p(T|P_1)}{dP_1} = I(P_1) (\hat{P}_1 - P_1), \quad (13)$$

with $I(P_1)$ as Fisher information matrix. In this case, the difference between \mathcal{H}_0 and \mathcal{H}_1 is P_1 . Therefore, $p(T|P_1, L_1, \mathcal{H}_1)$ is simplified and expressed as $p(T|P_1)$. Then, the first order Taylor series is used to expand $p(T|P_1)$, and the following equation can be obtained:

$$I(P_1) = I(\hat{P}_1) + \left. \frac{dI(P_1)}{dP_1} \right|_{P_1=\hat{P}_1} (P_1 - \hat{P}_1). \quad (14)$$

Substitute Eq. (14) into Eq. (13), and Eq. (13) can be expressed as

$$\frac{d \ln p(T|P_1)}{dP_1} = I(\hat{P}_1) (\hat{P}_1 - P_1) - \left. \frac{dI(P_1)}{dP_1} \right|_{P_1=\hat{P}_1} (P_1 - \hat{P}_1)^2. \quad (15)$$

Since the maximum likelihood estimation of transmitted power is consistent, that is, with the increase of the number of sample values, the estimated value approaches the true value. Therefore, the second-order components in Eq. (15) can be ignored. Then Eq. (15) can be written as

$$\frac{d \ln p(T|P_1)}{dP_1} = I(\hat{P}_1) (\hat{P}_1 - P_1). \quad (16)$$

By integrating both sides of Eq. (16) with respect to P_1 , Eq. 16 can be expressed as

$$\ln p(T|P_1) = -\frac{1}{2} I(\hat{P}_1) (\hat{P}_1 - P_1)^2 + C(\hat{P}_1). \quad (17)$$

Because the integral constant $C(\hat{P}_1) = \ln p(T|\hat{P}_1)$, the progressive form of $p(T|P_1)$ can be written as

$$p(T|P_1) = p(T|\hat{P}_1) \exp \left[-\frac{1}{2} I(\hat{P}_1) (\hat{P}_1 - P_1)^2 \right]. \quad (18)$$

Substitute it into Eq. (12), and GLRT test statistics can be simplified as

$$L_G(T) = \exp \left[\frac{1}{2} I(\hat{P}_1) (\hat{P}_1 - P_1)^2 \right]. \quad (19)$$

By using the monotonically increasing property of exponential function, the asymptotic form of GLRT can be expressed as

$$2 \ln L_G(T) = I(\hat{P}_1) (\hat{P}_1 - P_1)^2. \quad (20)$$

Combining Eq. (16), the final asymptotic detection statistics can be derived as

$$T_R(T) = \hat{P}_1 \left. \frac{d \ln p(T|P_1, L_1)}{dP_1} \right|_{P_1=0} \begin{matrix} d_H = \mathcal{H}_1 \\ > \\ < \\ d_H = \mathcal{H}_0 \end{matrix} \lambda_R, \quad (21)$$

where

$$\begin{aligned} \frac{d \ln p(T|P_1, L_1)}{dP_1} &= \sum_{k=1}^K \frac{d \ln p(T_k|P_{1,k})}{dP_1} \\ &= \sum_{k=1}^K \frac{d \ln p(T_k|P_{1,k})}{dP_{1,k}} \frac{dP_{1,k}}{dP_1}, \end{aligned} \quad (22)$$

with $\frac{dP_{1,k}}{dP_1}$ determined by the channel gain. It is easy to derive that when it comes to calculating $p(T|P_1, L_1)$, the channel model needs to be specified. The goal of the test is to determine whether the secondary user is working, so Eq. (21) has obvious physical significance. It can be known from the subsequent formula expansion that the derivative increases with the increase of T . If the secondary user is working, the value of T will be larger and the derivative will increase. At the same time, the estimated value of transmitted power will also increase. The product of derivative and amplitude approximates the probability when the user works. However, there is an approximation in this process, that is, the derivative of zero replaces the integral, thus simplifying the expression.

According to Eq. (21), it can determine whether the secondary user works or not. When a secondary user is detected, the secondary user in the primary user communication area can be directly asserted to have violated the interference constraint. If the secondary user is in the communication protection belt, it is necessary to evaluate whether the power used by the secondary user is in violation of regulations, namely the following binary hypothesis testing problem

$$\begin{cases} \mathcal{G}_0 : P_1 \leq P_a, \\ \mathcal{G}_1 : P_1 > P_a. \end{cases} \quad (23)$$

In view of the above detection problems, a similar detection method can be designed according to the detector that is determined to have or not. Intuitively, when determining whether the transmitted power of the secondary user exceeds the limit, it is faced with the compromise between detection probability and false alarm probability, and the highest false alarm probability occurs when the secondary user works normally with the maximum power assigned. Therefore, the detector is designed based on the worst-case, i.e.,

$$T_R(T) = (\hat{P}_1 - P_a) \left. \frac{d \ln p(T|P_1, L_1)}{dP_1} \right|_{P_1=P_a} \begin{matrix} d_G = \mathcal{G}_1 \\ > \\ < \\ d_G = \mathcal{G}_0 \end{matrix} \lambda_d, \quad (24)$$

where $d_G \in \{0(\mathcal{G}_0), 1(\mathcal{G}_1)\}$, with d_G as this detector's verdict, P_a as the maximum power assigned, λ_d as the decision threshold. In Eq. (24), $(\hat{P}_1 - P_a)$ is substituted for \hat{P}_1 in Eq. (21), and the derivative is set at $P_1 = P_a$. From the above equation, it can be seen that if the estimated value

of transmitted power is greater than the maximum power allocated, the coefficient in front is positive, and the product of the coefficient and the derivative determines whether the secondary user violates the interference constraint, otherwise it is negative, and the secondary user is judged not to violate the interference constraint. It can be concluded that the estimation of transmitted power has great influence on the accuracy of detection.

B. ESTIMATION OF THE SECONDARY USER'S TRANSMITTED POWER

In general, after the expansion of $\frac{d \ln p(T|P_1, L_1)}{d P_1} = 0$, it is very complex and difficult to make the estimation with low computational cost. Therefore, it is difficult to directly obtain the maximum likelihood estimation of the transmitted power. For this problem, the transmitted power of secondary users is inferred from the received power of each node, and the sub-optimal estimation of transmitted power is obtained. This is because it is relatively easy to obtain the closed solution of the maximum likelihood estimation of transmitted power at a single node.

First, at each node, the received power's estimation of the node is obtained by derivation, i.e.,

$$\frac{d \ln p(T_k|P_{1,k})}{d P_{1,k}} = 0. \tag{25}$$

It can be obtained after the simplification that

$$\mu_k^2 + M T_k \mu_k - M T_k^2 = 0, \tag{26}$$

where $\mu_k = P_{0,k} + P_{1,k} + N_k$, it follows that

$$\hat{P}_{1,k} = \frac{1}{2} M T_k + T_k \sqrt{\frac{1}{4} M^2 + M - P_{0,k} - N_k}. \tag{27}$$

Then, according to the estimated received power of each sensing node and the relative position of the node and the secondary user, the transmitted power [28] of the secondary user can be further estimated:

$$\hat{P}_1 = \frac{1}{\theta} \left(\prod_{k=1}^K \hat{P}_{1,k} d_{1,k}^\alpha \right)^{\frac{1}{K}}, \tag{28}$$

where $\theta = \frac{c}{4\pi f_c}$, with α as the path fading factor, c as the electromagnetic wave propagation velocity, f_c as the carrier frequency.

However, in the process of transmitted power's estimation, the estimation of received power made by the sensing node is a local optimization without comprehensive consideration of the relative position relationship between secondary users and other sensing nodes. Considering the worse case that the target user is not the actual working user, the final transmitted power is still calculated according to Eq. (28), and great error will be generated. Therefore, it is necessary to consider the received power estimation of the sensing nodes, the selection of the target user and the transmitted power estimation together. For the above problems, the received power at each node can be calculated according to Eq. (27), and different

secondary users can be selected in turn, from which the secondary users with the greatest posterior probability can be selected, i.e.,

$$\hat{L}_1 = \arg \max_{L \in S_L} \sum_k \ln p(T_k|L_1, f(\hat{P}_1, d_{1,k})), \tag{29}$$

where

$$f(\hat{P}_1, d_{1,k}) = C \hat{P}_1 \left(\frac{d_1}{d_{1,k}} \right)^\alpha, \tag{30}$$

with $f(\hat{P}_1, d_{1,k})$ as the power of a single node estimated from the secondary user's estimated transmitted power, S_L as the location information set of all secondary users, C as a unitless constant.

Finally, the position of the secondary user and the estimated transmitted power are substituted into Eq. (21) to determine the working status of the secondary user.

C. ICV DETECTION UNDER MULTIPLE SECONDARY USERS

Similar to the detection of a single secondary user, the detection of multiple secondary users essentially utilizes the idea of detection of a single secondary user, that is, detecting one by one rather than simultaneously. In the communication protection belt, different secondary users can work simultaneously at a certain distance to control mutual interference. Different from the scenario where a single secondary user works, when multiple secondary users work at the same time, the data difference of the sensing nodes will be more significant. In particular, for a specific node, in addition to the primary user signal, it will also receive signals from multiple secondary users, especially signals from the secondary users who are close to it. Therefore, for different secondary users, it is necessary to select different sensing nodes, especially those that are close to each other.

Meanwhile, in practice, the accuracy of detection results is not necessarily improved with the increase of the number of sensing nodes, but is closely related to the relative positions of sensing nodes, secondary users and primary users. On the one hand, according to the signal fading model, the smaller the distance between the sensing node and the secondary user, the greater the signal strength received by the secondary user. Therefore, it is more accurate to reflect the real working status of secondary users. In addition, the sensing nodes farther away from the secondary users are more susceptible to noise. For the detection of this secondary user, the data value of this sensing node is limited, even misleading the final judgment [29]. It is worth noting that in the communication area of the primary user, the sensing nodes will be strongly influenced by the primary user. In conclusion, the estimation of secondary users' transmitted power plays a key role in the detection of ICV. However, the sensing nodes that are far away from the secondary user, or those that are strongly influenced by the primary user, will lead to a larger power estimation error, that is, the power of the secondary user is often overestimated, thus causing a serious deviation in the estimation of transmitted power in Eq. (28).

Therefore, simply the location of sensing nodes cannot meet the needs of node selection.

According to the above observation, when there are multiple secondary users working at the same time, a sensing node selection mechanism based on SINR is designed from the perspective of reducing computational complexity, transmission overhead and improving detection accuracy. The reason why SINR is chosen as the basis of selection mechanism is that compared with simple position relation, SINR can well reflect the influence of secondary user's signal on the sensing data. Specifically, from the perspective of secondary user's detection, the mean SINR at the sensing node can be expressed as

$$SINR = \frac{p_1 \left(\frac{d_1}{d_{1,k}}\right)^\alpha}{p_0 \left(\frac{d_0}{d_{0,k}}\right)^\alpha + N_k}. \quad (31)$$

The received power p_1 at the reference position is the value to be estimated, however, the value is consistent for all the sensing nodes. Therefore, based on the node-selection mechanism of SINR, the set of nodes involved in detection and estimation can be obtained as

$$S_u = \left\{ k \mid \frac{1}{P_{0,k} + N_k} \left(\frac{d_0}{d_{1,k}}\right)^\alpha > \varepsilon \right\}, \quad (32)$$

where the threshold ε is a constant.

Therefore, the test statistic in Eq. (21) is re-expressed as

$$T_R(T) = \hat{P}_1 \sum_{k \in S_u} \frac{1}{|S_u|} \frac{d \ln p(T_k | P_1, L_1)}{dP_1} \Bigg|_{P_1 = \hat{P}_1}, \quad (33)$$

where $|S_u|$ represents the number of sensing nodes selected to participate in the detection of the secondary user behavior. Similarly, to determine whether the transmitted power of the detector exceeds the specified range, Eq. (24) can be reformulated as

$$T_R(T) = \left(\hat{P}_1 - P_a \right) \sum_{k \in S_u} \frac{1}{|S_u|} \frac{d \ln p(T_k | P_1, L_1)}{dP_1} \Bigg|_{P_1 = P_a} \begin{matrix} \mathcal{G}_1 \\ \geq \\ \lambda_d \\ \mathcal{G}_0 \end{matrix}. \quad (34)$$

D. DETECTION OF ICV UNDER DIFFERENT SIGNAL FADING MODELS

1) AMPLITUDE DECAY FUNCTION MODEL

Firstly, the Amplitude Attenuation Function (AAF) model [30] was considered. After the location and power of secondary users were determined, the channel gain between users and nodes was also determined. Specifically, when only path fading is considered, the received power at the node can be written as

$$P_{1,j} = p_1 \left(\frac{d_1}{d_{1,j}}\right)^\alpha = \frac{\theta P_1}{d_{1,j}^\alpha}. \quad (35)$$

Therefore, Eq. (22) can be expressed as (The progress of derivation is shown in appendix.)

$$\frac{d \ln p(T | P_1, L_1)}{dP_1} = \sum_{k=1}^K \left(\frac{MT_k^2}{\mu_k^3} - \frac{MT_k}{\mu_k^2} - \frac{1}{\mu_k} \right) \frac{\theta}{d_{1,j}^\alpha}. \quad (36)$$

Substitute Eq. (36) into Eq. (21), then the detection statistic under AAF channel model can be written as

$$\begin{aligned} T_A(T) &= \max_{L_1 \in S_L} \hat{P}_1 \sum_{k=1}^K \left(\frac{MT_k^2}{\mu_k^3} - \frac{MT_k}{\mu_k^2} - \frac{1}{\mu_k} \right) \frac{\theta}{d_{1,k}^\alpha} \Bigg|_{P_1 = \hat{P}_1} \\ &= \max_{L_1 \in S_L} \hat{P}_1 \sum_{k=1}^K \left(\frac{MT_k^2}{(P_{0,k} + N_k)^3} - \frac{MT_k}{(P_{0,k} + N_k)^2} \right) \frac{1}{d_{1,k}^\alpha}. \end{aligned} \quad (37)$$

2) SHADOW FADING MODEL

Next, we consider the more general channel model, i.e., the signal propagation under path fading and shadow fading. Therefore, the received power of the secondary user signal at the node is

$$P_{1,k} = p_1 \left(\frac{d_1}{d_{1,k}}\right)^\alpha e^{X_{1,k}}, \quad (38)$$

where $X_{1,k}$ represents shadow fading and obeys

$$X_{1,k} \sim \mathcal{N}(0, \sigma^2). \quad (39)$$

The multipath component is negligible here because its effect can be attenuated by broadband detection and multiple sampling values. Therefore, shadow fading obeys logarithmic normal distribution with variance σ_{dB} , which satisfies

$$\sigma = 0.1 \ln(10) \sigma_{dB}. \quad (40)$$

Therefore, the received signal strength $P_{1,k}$ obeys the following distribution

$$P_{1,k}(dBm) \sim N(\bar{P}_{1,k}(dBm), \sigma_{dB}^2), \quad (41)$$

where

$$\bar{P}_{1,k}(dBm) = p_1(dBm) - 10\alpha \log_{10}(d_{1,k}/d_1). \quad (42)$$

Therefore, according to [31],

$$\begin{aligned} f_{P_{1,k}|P_1}(P_{1,k}|L_1, P_1) &= \frac{10/\log(10)}{\sqrt{2\pi\sigma_{dB}^2}} \frac{1}{P_{1,k}} \\ &\times \exp \left[-\frac{b}{8} \left(\log \frac{d_{1,k}^2}{\tilde{d}_{1,k}^2} \right)^2 \right] \end{aligned} \quad (43)$$

where $b = \left(\frac{10\alpha}{\sigma_{dB} \log 10}\right)^2$, $d_{1,k} = \|L_1 - l_k\|$, with l_k as the location of the k th sensing node, $\tilde{d}_{1,k} = d_0 \left(\frac{p_0}{P_{1,k}}\right)^{1/\alpha}$ as the distance estimated by the received power. This paper only considers the block fading, i.e., within a single sensing

time slot, the channel gain is constant. Then the likelihood function can be written as

$$\ln p(T|P_1, L_1) = \sum_{k=1}^K \int_{P_{1,k} > 0} \ln p(T_k|P_{1,k}) p(P_{1,k}|P_1, L_1) dP_{1,k}. \quad (44)$$

The computational complexity of integral is relatively high. Therefore, based on the idea of likelihood ratio test, the final test statistic can be expressed as

$$\begin{aligned} T_s(T) &= \hat{P}_1 \frac{d \sum_{k=1}^K \max_{P_{1,k}} \ln [p(T_k|P_{1,k}) p(P_{1,k}|P_1, L_1)]}{dP_1} \Bigg|_{P_1=0} \\ &= \hat{P}_1 \frac{\sum_{k=1}^K \left[\max_{P_{1,k}} \ln p(T_k|P_{1,k}) p(P_{1,k}|P_1 + \Delta, L_1) - \max_{P_{1,k}} \ln p(T_k|P_{1,k}) p(P_{1,k}|P_1, L_1) \right]}{\Delta} \Bigg|_{P_1=0} \\ &= \hat{P}_1 \frac{\sum_{k=1}^K \left[\max_{P_{1,k}} \ln p(T_k|P_{1,k}) p(P_{1,k}|P_1 = \Delta, L_1) - \ln p(T_k|P_{1,k} = 0) \right]}{\Delta}, \end{aligned} \quad (45)$$

In the above equation, it is difficult to split and differentiate due to the existence of maximization. Therefore, the derivative is differentiated based on the definition of derivative.

E. EVALUATION OF DETECTION PERFORMANCE

According to the division of detector, in the first part, which is to detect whether the secondary user is working or not; in the second part, which is to determine whether the transmitted power of the secondary user violates the interference constraint, false alarm and miss detection always exist. Therefore, in general, for the detection of ICV, the final detection results are as follows:

- No secondary users in work was detected;
- Secondary user in work was detected, and the user’s spectrum usage behavior was further determined not to violate interference constraints;
- Secondary user in work was detected and the user’s frequency use behavior was further determined to violate the interference constraint.

Therefore, when a secondary user does not actually violate the interference constraint, there are two types of false alarms: when the secondary user is not working or working at a reasonable power, the secondary user is judged to be working and violating the interference constraint, and these two types of false alarms can be expressed as

$$P_{f0} = P(d_H = 1|\mathcal{H}_0) \quad P(d_G = 1|d_H = 1, \mathcal{H}_0), \quad (46)$$

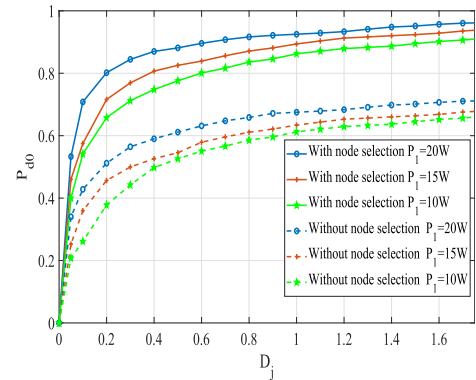


FIGURE 4. Performance of ICV detection in primary user communication area.

$$P_{f1} = P(d_H = 1|\mathcal{G}_0) \quad P(d_G = 1|d_H = 1, \mathcal{G}_0). \quad (47)$$

Similarly, when secondary user violates the interference constraint, there are two kinds of detection probability: secondary user working in the communication area is correctly detected, or secondary user working beyond the specified range of transmitted power is correctly detected. The two kinds of detection probability are respectively expressed as

$$P_{d0} = P(d_H = 1 | \|L_1 - L_0\| < D_p, \mathcal{H}_1), \quad (48)$$

$$P_{d1} = P(d_H = 1|\mathcal{G}_1) \quad P(d_G = 1|d_H = 1, \mathcal{G}_1). \quad (49)$$

IV. SIMULATION RESULTS AND ANALYSIS

A. SIMULATION SETUP

Equivalent isotropically radiated power (EIRP) is 62.7dBW. The transmitted power of the primary user is set to 37.15 W and the center frequency is 18.48 GHz. The single-point sensing slot length is 1 ms. The path fading factor is usually between 2 and 4, which is $\alpha = 3$ in this subsection. The signal propagation parameters are assumed to be known. The power limit for secondary users is 50 W. At the sensing node, the received noise power spectral density is -174 dBm/Hz, and the receiver noise factor is 11 dB. In the space-time spectrum sharing strategy considered in this paper, the signal-to-noise ratio at the edge of the communication area of the primary user, i.e., $D_p = 1750m$, is -4 dB. In addition, the upper limit of interference constraint at the edge of the communication area is -120 dBm. The following simulation results are the average of 10000 simulation results under 500 random topologies. Unless specifically pointed out, the number of sensing nodes is $K = 50$, and the overall sensing slot length within the randomly distributed communication area and protection belt is 100 ms.

B. PERFORMANCE OF ICV DETECTION IN PRIMARY USER COMMUNICATION AREA

In order to protect the normal reception of the primary user’s signal, secondary users are not allowed to access the channel in the communication area of the primary user. Fig. 4 shows the performance comparison between the detection scheme with node selection and the detection scheme without node selection when the secondary user violates the interference

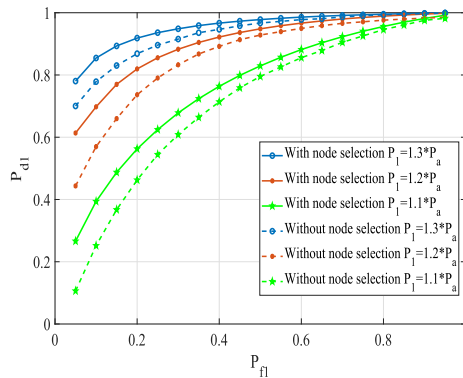


FIGURE 5. Performance of ICV detection in communication protection belt.

constraint and accesses the channel without permission. The false alarm probability of ICV detection is set as $P_{f0} = 0.1$. In the communication area of the primary user, the sensing nodes are greatly influenced by the signal of the primary user.

As the distance between the node and the primary user is shortened, the estimation error of transmitted power increases. Therefore, as shown in Fig. 4, when the secondary user is close to the primary user, the overall detection performance of the two schemes is poor because the sensing nodes are greatly affected by the primary user. However, with the increase of the distance, the performance of detection scheme with node selection is significantly improved, while the performance of the detection scheme without node selection is not. In addition, the higher the transmitted power of the secondary user is, the higher the received power at each node is, the higher the SINR is, and the higher the detection performance of the secondary user is. At this time, as the secondary user is in the communication area of the primary user, once the secondary user in the work is found, it can be judged as ICV. At the same time, it can be noted that when the secondary user is away from the primary user, the performance is gradually stable, because the influence of the primary user on the sensing nodes is relatively low. In general, the detection performance of the scheme with node selection is obviously better than that of the scheme without node selection, because the scheme based on node selection mechanism will not use too much useless data. So the detection performance is generally better than the detection scheme without node selection.

C. PERFORMANCE OF ICV DETECTION IN COMMUNICATION PROTECTION BELT

Different from the ICV detection in the communication area of the primary user, in the communication protection belt, it is not only necessary to detect the working secondary user, but also to further evaluate whether the secondary user works within the reasonable range of transmitted power.

As shown in Fig. 5, the working secondary user is detected to be 2.4km away from the primary user, and the reasonable upper limit of transmitted power at this position is $P_a = 37.7W$. False alarm probability P_{f1} in Fig. 5 is

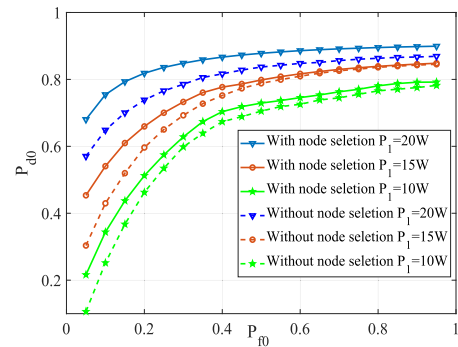


FIGURE 6. Relationship between P_{d0} and P_{f0} in primary user communication area.

the probability of misjudging secondary user’s violation of interference constraint when its transmitted power is P_a . There is a compromise between P_{d1} and P_{f1} . Compared with Fig. 4, it can be noted that the improvement of the detection performance is not quite significant because there is fewer impact on detection from primary user’s signal. However, the detection scheme with node selection really has a higher detection probability under the same false alarm constraint. At the same time, the larger the secondary user exceeds the reasonable power range, although the performance of the detection scheme without node selection and the scheme with node selection is gradually approaching, there is still some gap, which reflects the superiority of the node selection mechanism.

D. THE IMPACT OF FALSE ALARM DETECTION PROBABILITY ON THE DETECTION PERFORMANCE

The detection in this paper is divided into two parts, namely in the primary user communication area and the communication protection belt. The relationship between false alarm probability and detection performance in the communication protection belt is provided in the last subsection. Therefore, as shown in Fig. 6, we have added the relationship between false alarm probability and detection performance in the primary user communication area in this subsection. The working secondary user is detected to be 1km away from the receiver of primary user. Comparing the two curves, the performance of detection in the primary user communication area is inferior to it in the communication protection belt because of the impact of primary user’s signal. However, combining the two curves, we can conclude that under a certain false alarm constraint, the detection probability increases with the increase of false alarm probability.

E. THE INFLUENCE OF THE NUMBER OF SENSING NODES AND SAMPLES ON THE DETECTION PERFORMANCE

In Fig. 7, the secondary user located within the communication protection belt is operating at transmitted power $P_1 = 1.2P_a$ which beyond a reasonable range. The sensing nodes are distributed randomly in the whole region. The increase of the number of sensing nodes can not only improve the amount of data involved in the fusion, but also get closer to the secondary users with a higher probability, so as to obtain

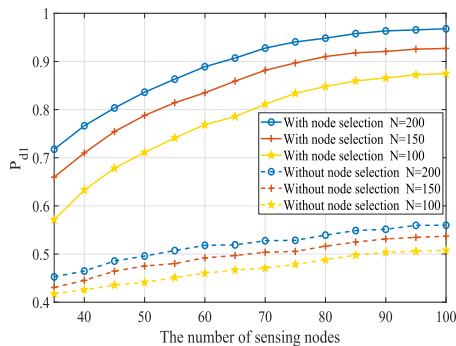


FIGURE 7. The influence of the number of sensing nodes and samples on detection performance.

more accurate spectrum information. The increase of sample number will directly improve the data quality of a single node and enhance the estimation accuracy of its received power. As shown in Fig. 7, when the number of sensing nodes and samples are improved in the detection scheme without node selection, the detection performance is slightly improved and even fluctuates, which is caused by the randomness of the distribution of the sensing nodes. However, the performance of the detection scheme with node selection is greatly improved compared with the former when the number of sensing nodes and samples are improved. Moreover, we have found that when the number of nodes exceeds 90, the detection probability would not be greatly improved (The slope of the curve is not increasing so much.). As we all know, detection performance is supposed to be positively correlated with the number of sensing nodes from the perspective of the data fusion, however, we cannot just consider improving detection performance without considering the cost. There should be a contradiction between the decrease of the computation costs, the devices' costs and the improvement of the detection performance. Therefore, from a practical point of view, people prefer to sacrifice some detection performance to reduce the cost. How to get the best detection probability under the constraint of a certain number of sensors might be a good deployment optimization problem in the future.

V. CONCLUSION

In this paper, we consider the heterogeneous spectrum sharing scenario that the primary user is the satellite system and the secondary user is the ground system. The detection of interference constraint violation is a critical but challenging issue in satellite-earth integrated networks. To address this problem, we propose a new geolocation spectrum database framework for tasks definition in the spectrum sharing and formulate a generalized model for spectrum sharing in the satellite-earth integrated networks. We propose detailed signal detection and estimation strategies to detect the working status of secondary user in the downlink spectrum sharing scenario. Furthermore, we derive the closed-form for test statistics. According to the status and transmitted power of secondary user, we can determine whether the secondary user has violated the interference constraint. Simulation examples are provided to verify the proposed studies.

APPENDIX

First of all, Eq. (20) can be expressed as

$$\begin{aligned} \frac{d \ln p(T|P_1, L_1)}{dP_1} &= \sum_{k=1}^K \frac{d \ln p(T_k|P_{1,k})}{dP_1} \\ &= \sum_{k=1}^K \frac{d \ln p(T_k|P_{1,k})}{dP_{1,k}} \frac{dP_{1,k}}{dP_1} \end{aligned} \quad (50)$$

Then, based on the distribution of T_k , $\frac{d \ln p(T_k|P_{1,k})}{dP_{1,k}}$ can be re-expressed as follows:

$$\begin{aligned} &\frac{d \ln \left\{ \frac{1}{\sqrt{2\pi} \frac{\mu_k^2}{M}} \exp \left[-\frac{(T_k - \mu_k)^2}{2 \frac{\mu_k^2}{M}} \right] \right\}}{dP_{1,k}} \\ &= \frac{d \left[-\frac{1}{2} \ln 2\pi \frac{\mu_k^2}{M} - \frac{M}{2} \frac{(T_k - \mu_k)^2}{\mu_k^2} \right]}{dP_{1,k}} \\ &= -\frac{1}{2} \frac{\frac{2\pi}{M} \cdot 2\mu_k}{2\pi \cdot \frac{\mu_k^2}{M}} - \frac{M}{2} \cdot \frac{2(\mu_k - T_k) \mu_k^2 - 2\mu_k(T_k - \mu_k)^2}{\mu_k^4} \\ &= -\frac{1}{\mu_k} - M \left(\frac{\mu_k - T_k}{\mu_k^2} - \frac{\mu_k^2 - 2\mu_k T_k + T_k^2}{\mu_k^3} \right) \\ &= \frac{MT_k^2}{\mu_k^3} - \frac{MT_k}{\mu_k^2} - \frac{1}{\mu_k} \end{aligned} \quad (51)$$

Finally, substitute Eq. (50) into Eq. (51), we can get Eq. (36).

REFERENCES

- [1] S. Haykin, "Cognitive radio: Brain-empowered wireless communications," *IEEE J. Sel. Areas Commun.*, vol. 23, no. 2, pp. 201–220, Feb. 2005.
- [2] J. Mitola and G. Q. Maguire, "Cognitive radio: Making software radios more personal," *IEEE Pers. Commun.*, vol. 6, no. 4, pp. 13–18, Aug. 1999.
- [3] D. Niyato, E. Hossain, and Z. Han, "Dynamic spectrum access in IEEE 802.22-based cognitive wireless networks: A game theoretic model for competitive spectrum bidding and pricing," *IEEE Wireless Commun.*, vol. 16, no. 2, pp. 16–23, Apr. 2009.
- [4] H. Li, Q. Guo, and Q. Li, "Satellite-based multi-resolution compressive spectrum detection in cognitive radio networks," in *Proc. 2nd Int. Conf. Instrum., Meas., Comput., Commun. Control*, Dec. 2012, pp. 1081–1085.
- [5] Z. Li, D. Wang, P. Qi, and B. Hao, "Maximum-Eigenvalue-Based sensing and power recognition for multiantenna cognitive radio system," *IEEE Trans. Veh. Technol.*, vol. 65, no. 10, pp. 8218–8229, Oct. 2016.
- [6] M. Ju and K.-M. Kang, "Cognitive radio networks with secondary network selection," *IEEE Trans. Veh. Technol.*, vol. 65, no. 2, pp. 966–972, Feb. 2016.
- [7] C. Zhang, C. Jiang, J. Jin, S. Wu, L. Kuang, and S. Guo, "Spectrum sensing and recognition in satellite systems," *IEEE Trans. Veh. Technol.*, vol. 68, no. 3, pp. 2502–2516, Mar. 2019.
- [8] C. Zhang, C. Jiang, L. Kuang, J. Jin, Y. He, and Z. Han, "Spatial spectrum sharing for satellite and terrestrial communication networks," *IEEE Trans. Aerosp. Electron. Syst.*, vol. 55, no. 3, pp. 1075–1089, Jun. 2019.
- [9] G. Ding, J. Wang, Q. Wu, F. Song, and Y. Chen, "Spectrum sensing in opportunity-heterogeneous cognitive sensor networks: How to cooperate?" *IEEE Sensors J.*, vol. 13, no. 11, pp. 4247–4255, Nov. 2013.
- [10] Z. Wang, X. Wan, Z. Fan, and M. Wang, "Optimal power control in cognitive radio networks under interference power constraint and quality of service constraints," in *Proc. IEEE Int. Conf. Commun. Syst. (ICCS)*, Dec. 2016, pp. 1–5.
- [11] Y.-C. Liang, Y. Zeng, E. Peh, and A. T. Hoang, "Sensing-throughput tradeoff for cognitive radio networks," in *Proc. IEEE Int. Conf. Commun.*, Jun. 2007, pp. 1326–1337.

- [12] Q. Wu, G. Ding, J. Wang, and Y.-D. Yao, "Spatial-temporal opportunity detection for spectrum-heterogeneous cognitive radio networks: two-dimensional sensing," *IEEE Trans. Wireless Commun.*, vol. 12, no. 2, pp. 516–526, Feb. 2013.
- [13] L. Zhang, G. Ding, Q. Wu, and Z. Han, "Spectrum sensing under spectrum misuse behaviors: A multi-hypothesis test perspective," *IEEE Trans. Inf. Forensics Security*, vol. 13, no. 4, pp. 993–1007, Apr. 2018.
- [14] L. Zhang, G. Ding, and Q. Wu, "Detecting abnormal power emission for orderly spectrum usage," *IEEE Trans. Veh. Technol.*, vol. 68, no. 2, pp. 1989–1992, Feb. 2019.
- [15] M. Haghighat and S. M.-S. Sadough, "Cooperative spectrum sensing in cognitive radio networks under primary user emulation attacks," in *Proc. 6th Int. Symp. Telecommun. (IST)*, Nov. 2012, pp. 2135–2141.
- [16] B. Mark and A. Nasif, "Estimation of maximum interference-free power level for opportunistic spectrum access," *IEEE Trans. Wireless Commun.*, vol. 8, no. 5, pp. 2505–2513, May 2009.
- [17] R. Menon, R. M. Buehrer, and J. H. Reed, "Outage probability based comparison of underlay and overlay spectrum sharing techniques," in *Proc. 1st IEEE Int. Symp. New Frontiers Dyn. Spectr. Access Netw. (DySPAN)*, Nov. 2005, pp. 101–109.
- [18] J. Unnikrishnan and V. V. Veeravalli, "Cooperative sensing for primary detection in cognitive radio," *IEEE J. Sel. Topics Signal Process.*, vol. 2, no. 1, pp. 18–27, Feb. 2008.
- [19] S. Kandeepan, L. De Nardis, M.-G. Di Benedetto, A. Guidotti, and G. E. Corazza, "Cognitive satellite terrestrial radios," in *Proc. IEEE Global Telecommun. Conf. GLOBECOM*, Dec. 2010, pp. 1–6.
- [20] S. K. Sharma, S. Chatzinotas, and B. Ottersten, "Satellite cognitive communications: Interference modeling and techniques selection," in *Proc. 6th Adv. Satell. Multimedia Syst. Conf. (ASMS)*, Sep. 2012, pp. 111–118.
- [21] R. Murty, R. Chandra, T. Moscibroda, and P. Bahl, "SenseLess: A database-driven white spaces network," *IEEE Trans. Mobile Comput.*, vol. 11, no. 2, pp. 189–203, Nov. 2012.
- [22] G. Ding, J. Wang, Q. Wu, Y.-D. Yao, F. Song, and T. A. Tsiftsis, "Cellular-base-station-assisted device-to-device communications in TV white space," *IEEE J. Sel. Areas Commun.*, vol. 34, no. 1, pp. 107–121, Jan. 2016.
- [23] M. Höyhtyä, A. Mämmelä, X. Chen, A. Hukkoniemi, J.-C. Dunat, and J. Gardy, "Database-assisted spectrum sharing in satellite communications: A survey," *IEEE Access*, vol. 5, pp. 25322–25341, 2017.
- [24] *Series of ITU Recommendations Propagation by Diffraction*, document I.-R. P.526-8, Nov. 2013.
- [25] *Satellite Antenna Radiation Pattern for Use as a Design Objective in the Fixed-Satellite Service Employing Geostationary Satellites*, document I.-R. S.672-4, Jan. 2010.
- [26] A. W. Min, X. Zhang, and K. G. Shin, "Detection of small-scale primary users in cognitive radio networks," *IEEE J. Sel. Areas Commun.*, vol. 29, no. 2, pp. 349–361, Feb. 2011.
- [27] S. Jana and S. K. Kasper, "On fast and accurate detection of unauthorized wireless access points using clock skews," *IEEE Trans. Mobile Comput.*, vol. 9, no. 3, pp. 449–462, Mar. 2010.
- [28] M. Zafer, B. Ko, and I. W.-H. Ho, "Cooperative transmit-power estimation under wireless fading," in *Proc. 9th ACM Int. Symp. Mobile Netw. Comput.*, 2008, pp. 381–390.
- [29] A. Dutta and M. Chiang, "'See something, say something' crowdsourced enforcement of spectrum policies," *IEEE Trans. Wireless Commun.*, vol. 15, no. 1, pp. 67–80, Aug. 2015.
- [30] D. Ciuonzo, P. S. Rossi, and P. Willett, "Generalized Rao test for decentralized detection of an uncooperative target," *IEEE Signal Process. Lett.*, vol. 24, no. 5, pp. 678–682, May 2017.
- [31] N. Patwari, A. O. Hero, M. Perkins, N. S. Correal, and R. J. O'Dea, "Relative location estimation in wireless sensor networks," *IEEE Trans. Signal Process.*, vol. 51, no. 8, pp. 2137–2148, Aug. 2003.



NING YANG received the B.S. degree in communication engineering from Xidian University, Xi'an, China, in 2018. He is currently pursuing the M.S. degree in information and communication engineering with the College of Communications Engineering, Army Engineering University of PLA, Nanjing, China. His research interests include satellite communication, spectrum sensing, deep learning, and signal detection and estimation.



PINGHUI LI received the B.Eng. and M.Eng. degrees in electrical engineering from the Institute of Communications Engineering (ICE), Nanjing, China. He has authored or coauthored more than 30 conference and journal articles. His research interests include microwave circuit, antenna, and computational electromagnetics.



DAOXING GUO (Member, IEEE) received the B.S., M.S., and Ph.D. degrees from the Institute of Communications Engineering (ICE), Nanjing, China, in 1995, 1999, and 2002, respectively. He is currently a Full Professor and a Ph.D. Supervisor with the PLA University of Science and Technology. He has authored or coauthored more than 40 conference and journal articles. He has been granted over 20 patents in his research areas. His current research interests include satellite communications systems and transmission technologies, communication anti-jamming technologies, and communication anti-interception technologies, including physical layer security and so on. He has served as a Reviewer for several journals in the communication field.



LINYUAN ZHANG received the B.S. degree (Hons.) in electronic engineering from Inner Mongolia University, Hohhot, China, in 2012, and the M.S. degree (Hons.) and Ph.D. degree (Hons.) in communications and information system from the College of Communications Engineering, PLA University of Science and Technology, in 2015 and 2018, respectively. He is currently a Research Assistant with the Jiangnan Institute of Computing Technology. His research interests include cognitive radio networks and anomaly detection.



GUORU DING (Senior Member, IEEE) received the B.S. degree (Hons.) in electrical engineering from Xidian University, Xi'an, China, in 2008, and the Ph.D. degree (Hons.) in communications and information systems from the College of Communications Engineering, Nanjing, China, in 2014.

From 2015 to 2018, he was a Postdoctoral Research Associate with the National Mobile Communications Research Laboratory, Southeast University, Nanjing. He is currently an Associate Professor with the College of Communications Engineering, Army Engineering University of PLA, Nanjing. His research interests include cognitive radio networks, massive MIMO, machine learning, and data analytics over wireless networks. He was a recipient of the Natural Science Foundation for Distinguished Young Scholars of Jiangsu Province, China, and six best paper awards from international conferences, such as the IEEE VTC-FALL 2014. He has received the Excellent Doctoral Thesis Award of the China Institute of Communications, in 2016, the Alexander von Humboldt Fellowship, in 2017, the Excellent Young Scientist of Wuwenjun Artificial Intelligence, in 2018, and the 14th IEEE COMSOC Asia-Pacific Outstanding Young Researcher Award, in 2019. He has served as a Guest Editor for the IEEE JOURNAL ON SELECTED AREAS IN COMMUNICATIONS—Special Issue on Spectrum Sharing and Aggregation in Future Wireless Networks. He is also an Associate Editor of the IEEE TRANSACTIONS ON COGNITIVE COMMUNICATIONS AND NETWORKING and a Technical Editor of the IEEE 1900.6 Standard Association Working Group.

• • •